Composite Structures 94 (2012) 3321–3326

Contents lists available at SciVerse ScienceDirect

Composite Structures

journal homepage: www.elsevier.com/locate/compstruct

# Optimization of composite stiffened panels under mechanical and hygrothermal loads using neural networks and genetic algorithms

L. Marín [a], D. Trias [a,*], P. Badalló [a], G. Rus [b], J.A. Mayugo [a]

[a] AMADE, Dept. of Mechanical Engineering and Industrial Construction, Universitat de Girona, Campus Montilivi s/n, E-17071 Girona, Spain
[b] Dept. of Structural Mechanics, Universidad de Granada, Politécnico de Fuentenueva, E-18071 Granada, Spain

A R T I C L E I N F O

*Article history:*
Available online 23 May 2012

*Keywords:*
Multi-objective optimization
Hygrothermal effects
Stiffened panels
Neural networks
Genetic algorithms
Finite element method

A B S T R A C T

The present work develops an optimization procedure for a geometric design of a composite material stiffened panel with conventional stacking sequence using static analysis and hygrothermal effects. The procedure is based on a global approach strategy, composed by two steps: first, the response of the panel is obtained by a neural network system using the results of finite element analyses and, in a second step, a multi-objective optimization problem is solved using a genetic algorithm. The neural network implemented in the first step uses a sub-problem approach which allows to consider different temperature ranges. The compression load and relative humidity of the air are assumed to be constants throughout the considered temperature range.

The mass, the hygrothermal expansion and the stresses between the skin and the stiffeners are defined as the optimality criteria. The presented optimization procedure is shown to yield the optimal structure design without compromising the computational efficiency.

© 2012 Elsevier Ltd. All rights reserved.

## 1. Introduction

Fibre reinforced polymer (FRP) composite materials have been used in the aerospace industry because of their high strength-to-weight and stiffness-to-weight ratios, and good behavior under elevated temperature environments. However, the major drawback of these materials is its high cost, so a suitable design and optimization process is essential in order to improve their structural behavior to cost ratio.

This has led several authors to study the optimization of composite panels, considering frequently as an objective the minimum mass, by geometric [1–3] and stacking sequence design [4–11]. On the other hand, these studies have focused on buckling or post-buckling dynamic analysis, without considering environmental effects. Nevertheless, these structures are exposed to extreme environmental conditions and some researchers have studied optimization problems of laminated composite plates with thermal effects to maximize the critical temperature capacity with uniform [12,13] or nonuniform temperature distribution [14]. In addition, Ijsselmuiden et al. [15] carried out a thermomechanical design optimization of composite panels and Cho [16] studied the hygrothermal effects in optimization problems of dynamic behavior, where temperature and moisture are assumed to be uniform once they have reached equilibrium.

Moisture and temperature changes affect the stiffness and strength of composites, and generate tensions between bonded sub-components. Their static and dynamic behaviors can depend significantly on such hygrothermal conditions. The combination of both phenomena is usually known as hot-wet (H/W) conditions. This state is characterized by moisture absorption by the matrix due its exposure to humid air and high temperature, which reduces the mechanical properties of the laminate. Additionally, this absorption causes a volume increase and consequently internal tensions between elements and interfaces. Experimental results show the influence of the temperature in moisture absorption [17–20], so this phenomenon should be analyzed for different thermal load cases and hygrothermal effects should be considered in any design and optimization process. On the other hand, Orifici et al. [21,22] analyzed the post-buckling failure of T-shaped stringers classifying in four failure modes: bend, blade, flange and core failure. The authors also found that delamination arises under the edges of stiffeners and the triangular resin-rich area.

The solution of the optimization problem is generally obtained with genetic algorithms (GAs) which have become one of the most employed solution method in engineering problems since they can handle integer, zero-one, discrete and continuous variables and are effective with nonlinear functions and non-convex design spaces. Due to this, both geometric and stacking sequence variables can be introduced. These methods are based on Darwin's theory of natural adaptation and biological evolution [23,24], which is translated into algorithmic terms through the computational

* Corresponding author.
*E-mail address:* dani.trias@udg.edu (D. Trias).

0263-8223/$ - see front matter © 2012 Elsevier Ltd. All rights reserved.
http://dx.doi.org/10.1016/j.compstruct.2012.04.024

operators of selection, crossover and mutation. In engineering applications, the evaluation of the objective function may be performed by means of an analytical function or, frequently, a numerical model (a finite element model, for instance). Since a large number of evaluations is generally required to obtain the optimal solution, the whole solution process implies a high computational cost. Some authors have used global approximation techniques to reduce function evaluation computational time by using data previously obtained with analytical or numerical methods. In this direction, Bisagni and Lanzi [25] developed an optimization procedure with a global approximation strategy based on obtaining the structure response by means of a system of artificial neural networks (ANNs) and GA. Lanzi et al. [26] performed a comparative study between three different global approximation techniques: ANN, kriging method and radial basis functions. All the techniques showed a similar behavior that the dynamic finite element (FE) analysis and computational time was satisfactorily reduced.

The aim of the present work is the definition of a fast multi-objective optimization procedure for the geometric design of stiffened panels under mechanical and hygrothermal loads, which minimizes the mass, the stresses between elements and the strain due to hygrothermal effects. The optimization problem is subject, in turn, to the corresponding constraints of tensions between stiffener-skin, provided by a failure criterion. The optimization procedure is carried out under different thermal load cases. A global approximation technique based on ANN is used to reduce computational cost.

This paper is structured as follows: firstly, in Section 2, a standard panel is analyzed to set up the model that will compute the objective functions and to define suitable constraints; the optimization process is described in Section 3; next, results are shown in Section 4 and finally, conclusions are presented in Section 5.

## 2. Definition of the multi-objective problem

### 2.1. Stiffened panel design

The considered structure is a compression loaded stiffened composite panel with three stringers, as shown in Fig. 1. This kind of panels represents a flat and partial idealization of the wings and fuselage structures of commercial aircrafts and so is frequently used in analysis and testing as a subcomponent. It is made of carbon fiber reinforced polymer (CFRP) and is symmetric in $x$–$z$ and $y$–$z$ planes. The stiffener sections are double-L shaped showing rounded corners with a mean radius of 4 mm for construction reasons. No run-outs are present. The different stacking sequences corresponding to each part of the geometry are shown in Fig. 1. Ply thickness is 0.184 mm. The specimen studied in this work is made with Hexcel T800/M21 prepeg ribbon of epoxy matrix reinforced with unidirectional carbon fibers. Its properties are shown in Table 1. The parametric analysis of the stiffened panel is performed in function of three geometric design variables $\mathbf{x} = (x_1, x_2, x_3)$ where $x_1$ is the stringer base width, $x_2$ is the stringer rib and $x_3$ is the distance between stringers with domains set forth in Table 2 and $\mathbf{x} \in \Omega_d$, where $\Omega_d$ is the decision space.

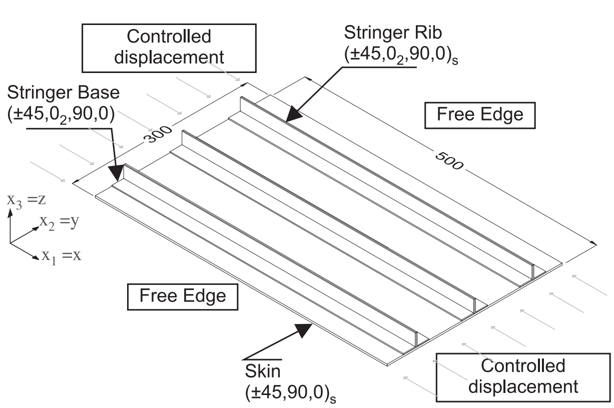


**Fig. 1.** Stiffened panel (dimensions in mm).

**Table 1**
T800/M21 UD CFRP properties [29].

| Property | Value | Description |
|---|---|---|
| $E_{xx}$ (GPa) | 134.7 | Young's modulus |
| $E_{yy} = E_{zz}$ (GPa) | 7.7 | |
| $\nu_{xy} = \nu_{xz}$ | 0.369 | Poisson's ratio |
| $\nu_{yz}$ | 0.5 | |
| $G_{xy} = G_{xz}$ (GPa) | 4.2 | Shear modulus |
| $G_{yz}$ (GPa) | 2.5 | |
| $\alpha_{xx}$ (°C$^{-1}$) | $-3.08 \times 10^{-7}$ | Coefficient of thermal expansion[a] |
| $\alpha_{yy} = \alpha_{zz}$ (C$^{-1}$) | $3.18 \times 10^{-5}$ | |
| $\rho$ (kg/m$^3$) | 1590 | Density |
| $X_T$ (MPa) | 2290.5 | Longitudinal tensile strength |
| $X_C$ (MPa) | 1051 | Longitudinal compression strength |
| $Y_T$ (MPa) | 41.43 | Transverse tensile strength |
| $Y_C$ (MPa) | 210 | Transverse compression strength |
| $S_L$ (MPa) | 69.4 | Shear strength |
| $S_{IS}$ (MPa) | 106.48 | Shear strength *in situ* |
| $\alpha$ (°) | 53.5 | Transverse compression fracture angle |
| $\beta$ | $5.10^{-8}$ | Shear response factor |
| $g$ | 0.5769 | Toughness ratio ($G_I/G_{II}$) |

[a] Values obtained using the relations described in [36].

**Table 2**
Geometric variables domain (mm).

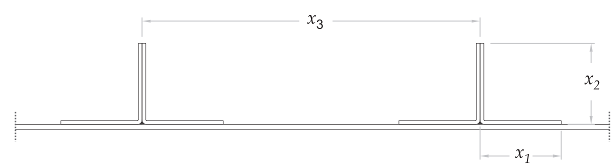


| Geometric variables: $\mathbf{x}$ | Lower bound: $\mathbf{x}^{(l)}$ | Upper bound: $\mathbf{x}^{(u)}$ |
|---|---|---|
| $x_1$: Stringers base width | 20 | 30 |
| $x_2$: Stringers rib | 20 | 30 |
| $x_3$: Stringers separation | 70 | 110 |

### 2.2. Model of the panel: finite element modeling

For the automatic parametric generation of panels, a *python* code is used together with the commercial software ABAQUS [27]. The stiffened panels are modeled by 4-node shells S4R, with six degree of freedom at each node, three integration points along the thickness for each ply. A compressive controlled displacement is applied to each transverse edge, while the longitudinal edges are free, as shown in Fig. 1. On the other hand, different temperature states are considered with a constant moisture.

The temperature and moisture are assumed to be in equilibrium state. The thermal strain is defined as $\epsilon^T = \alpha\Delta T$ and the moisture strain has been computed by the formulation proposed by Chang et al. [20] which considers the influence that temperature has in moisture strain for HTA1200A/ACD8801 material:

$$\epsilon^H = \frac{0.591R}{T + 273} \tag{1}$$

where $T$ is considered as the final temperature of the $\Delta T$ and $R$ is the relative humidity. This approach is used for transverse and out-of-

**Table 3**
Loading conditions for each subproblem.

| Subproblem ($n$) | Loading conditions | | | | |
|---|---|---|---|---|---|
| | Mechanical: compression controlled displacement | Moisture content ($H$ [%]) | Thermal ($T$[°C]) | | |
| | | | $T_I(y_1)$[a] | $T_F$[b] | $\Delta T(y_2)$[c] |
| SP1 | | | −55 | 120 | 175 |
| SP2 | | | 20 | 120 | 100 |
| SP3 | | | 70 | 90 | 20 |
| SP4 | 1.9 mm | 70 | 20 | −55 | −75 |
| SP5 | | | 70 | 20 | −50 |
| SP6 | | | 90 | −55 | −145 |
| SP7 | | | 120 | −70 | −50 |

[a] Initial temperature.
[b] Final temperature.
[c] Temperature variation.

plane direction, while the longitudinal moisture strain is considered negligible [28]. So the general form of stress–strain relationship for a transversely isotropic ply in which temperature and moisture effects are considered is $\epsilon^{\mathrm{Tot}} = \epsilon^{\mathrm{T}} + \epsilon^{\mathrm{H}} + \epsilon$, where the components are:

$$\begin{Bmatrix} \epsilon_{xx}^{\mathrm{Tot}} \\ \epsilon_{yy}^{\mathrm{Tot}} \\ \epsilon_{zz}^{\mathrm{Tot}} \end{Bmatrix} = \begin{Bmatrix} \alpha_{xx} \\ \alpha_{yy} \\ \alpha_{zz} \end{Bmatrix} \Delta T + \begin{Bmatrix} \approx 0 \\ \frac{0.591R}{T+273} \\ \frac{0.591R}{T+273} \end{Bmatrix} + \begin{Bmatrix} \epsilon_{xx} \\ \epsilon_{yy} \\ \epsilon_{zz} \end{Bmatrix} \tag{2}$$

A standard stiffened-panel, analyzed in a previous project [29], is taken as the reference panel with the following dimensions: $x_1$ = 24 mm, $x_2$= 24 mm and $x_3$= 100 mm. The behavior of the reference panel under different compressive and hygrothermal loads is studied in depth, using LaRC-03 failure criterion [30], which defines the following variables: failure indexes for transverse tensile failure ($FI_{\mathrm{TT}}$), transverse compressive failure ($FI_{\mathrm{TC}}$), longitudinal tensile failure ($FI_{\mathrm{LT}}$), and longitudinal compression failure ($FI_{\mathrm{LC}}$).

For temperature rising cases, the strains in the perpendicular direction are higher than the temperature decreasing cases, and localized in the stiffener bases, so the tensions between stringers and skin also increase. However, $FI_{\mathrm{TC}}$ and $FI_{\mathrm{LC}}$ indicate that the panel is capable of supporting larger temperature increases without breaking up to 1.45 mm compressive controlled displacement.

For decreasing thermal variations, the panel shows lower tensions, breaking with variations between −50° and −125° and compressive moderated displacement, depending on the final temperature. In these cases, $FI_{\mathrm{TT}}$ and $FI_{\mathrm{LC}}$ are the most important failure indexes. The interaction between moisture and thermal effects helps to the behavior of the panel but the matrix is damaged after the moisture absorption. Different environmental conditions with decreasing and rising thermal variations have been considered in the optimization problem.

### 2.3. Definition of subproblems

The behavior of the panel under a wide range of temperatures leading to different failure modes is analyzed. For this purpose, the initial problem has been decomposed into seven sub-problems so that, for each one, different ranges of temperature are considered. Initial temperatures correspond to the most significant values used in experimental analysis (generally −55 °C, ambient temperature, 70 °C, 90 °C and 120 °C) and temperature variations are chosen by the most important cases within the considered temperature range from −55° to 120° [31], where the minimum and the maximum service temperature commercial transport aircraft are considered as −54 °C and 71 °C respectively and the design ultimate loads at temperature up during takeoff and landing is 93 °C; the temperatures higher than 100 °C are considered only for special cases, such as supersonic transport, fighter, and bomber aircraft. So the different subproblems described in Table 3 were considered. The variables $T_I$ (initial temperature) and $\Delta T$ (temperature variation) form the vectors $\mathbf{y}_n = (y_{1n}, y_{2n})$ where $n$ is the number of each subproblem.

### 2.4. Formulation of the multi-objective optimization problem

A multi-objective problem is established, which seeks to minimize the weight of the panel $f_1(\mathbf{x}, \mathbf{y}_n)$, the local strain in direction perpendicular $f_2(\mathbf{x}, \mathbf{y}_n)$ and the tension between skin and stiffeners $f_3(\mathbf{x}, \mathbf{y}_n)$. All three objective functions are considered to be equally important.

In this way, the optimization problem can be formulated as:

$$\begin{array}{lll} \text{Minimize} & Y(f_1(\mathbf{x},\mathbf{y}_n), f_2(\mathbf{x},\mathbf{y}_n), f_3(\mathbf{x},\mathbf{y}_n)) & Y \in \Omega_o \\ \text{Subjectto} & g_k(\mathbf{x},\mathbf{y}_n) > 0 & k = 1,2 \\ & x_j^{(l)} \leqslant x_j \leqslant x_j^{(u)} & \\ \text{where} & \mathbf{y}_n = (y_{1n}, y_{2n}) & \\ & \mathbf{x} = (x_1, x_2, x_3) & \end{array} \tag{3}$$

where $\Omega_o$ is the objective space. The constraints $g_k(\mathbf{x}, \mathbf{y}_n)$ are defined as:

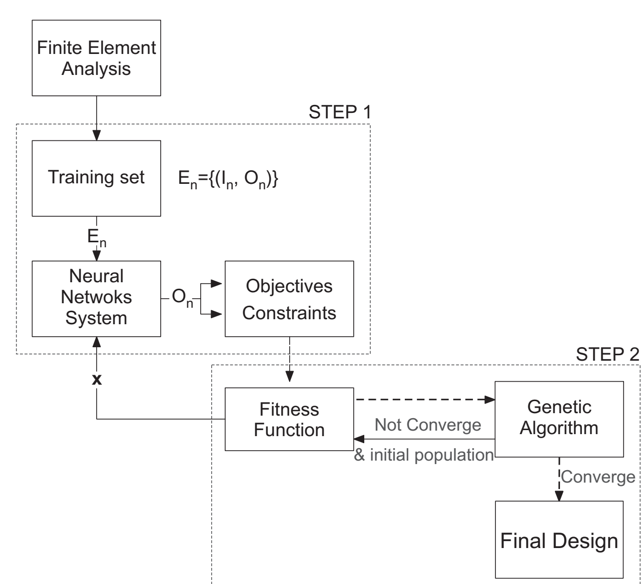


**Fig. 2.** Optimization scheme.

$$\left.\begin{aligned} g_1(\mathbf{x},\mathbf{y}_n) &= 1 - FI_{TC}(\mathbf{x},\mathbf{y}_n) \\ g_2(\mathbf{x},\mathbf{y}_n) &= 1 - FI_{LC}(\mathbf{x},\mathbf{y}_n) \end{aligned}\right\} \text{if } \Delta T > 0, \quad \left.\begin{aligned} g_1(\mathbf{x},\mathbf{y}_n) &= 1 - FI_{TT}(\mathbf{x},\mathbf{y}_n) \\ g_2(\mathbf{x},\mathbf{y}_n) &= 1 - FI_{LC}(\mathbf{x},\mathbf{y}_n) \end{aligned}\right\} \text{if } \Delta T < 0 \tag{4}$$

## 3. Optimization procedure

The solution of the problem, displayed in Eqs. (3) and (4), implies a high computational cost for the optimization process since the values of the objective functions and the constraints are obtained from a parametrized FE model. For this reason, the procedure shown in Fig. 2 based on a global approximation technique is used to reduce the computational time. This procedure is composed by two steps:

1. A system of ANN that is partially capable to reproduce the solution of the FE model is developed. To the seven inputs corresponding to each subproblem $E_n(I_n)$ it delivers the different outputs composed of the objectives and constraints $E_n(O_n)$.
2. A GA obtains to get the optimal value for the design variables previously described.

### 3.1. Model of the panel: neural network modeling

An ANN is a system used for information processing whose basic unit is inspired by the fundamental cell of the human nervous system: the neuron. This system is capable of acquiring knowledge and resolve situations that cannot be expressed mathematically by the experience [32].

The ANN needs a learning process and a training set, composed of input–output patterns, as known examples. The input signals of an artificial neuron are continuous variables instead of discrete pulses, as presented in a biological neuron. Each input signal passes through a *weight or gain*, known as *synaptic weight* or strength of the connection whose function is analogous to the *synaptic function* of the biological neuron. An other term, called *bias*, supposes a reinforcement of these connections. The summation node accumulates all input signals multiplied by the weights and bias and output passes through a *transfer function* or, where appropriate, *activation function*. The result of this sum is known as *propagation function*, which obtains the output vector.

A commercial software, MATLAB [33], was applied for developing an ANN procedure that includes the following process:

(a) *Choice of data set.* The training data set is composed by seven subsets that correspond to the different sub-problems displayed in Table 3. The set consists of an input–output pattern-pairs obtained through FE analysis.
The input pattern forms a vector $I_n$, composed of the geometrical parameters $\mathbf{x}$ and the vector $\mathbf{y}_n$, and the output pattern $O_n$, composed of the corresponding responses of the panel for each sub-problem (objectives and constraints).

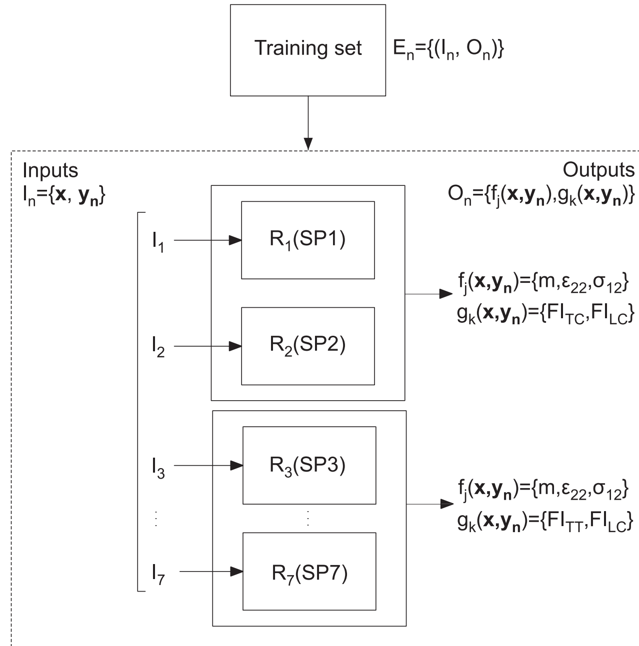


**Fig. 3.** Neural network scheme.

(b) *Architecture of the ANN.* The complexity of the problem is solved by using by a suitable architecture to implement the information of the input–output pattern for each subproblems discussed that, once inside the network will be merged.
This architecture, shown in Fig. 3, is defined by multilayer perceptron (MLP) that consists of an input layer with a vector dimensions $I_n$, two hidden layers with *compet* and *tansig* functions as *activation and transfer functions* respectively, and Levenberg–Marquardt [34] backpropagation learning rule and an output layer, with *tansig* function, that obtains the vector $O_n$, calculated from the bias and weights are adapted after training in the network.

(c) *Training of the ANN.* The ANN is taught to form the relationship between input and output variables by the training data set of known input–output patterns. This set is composed by

**Table 4**
Objectives and constraints values for each subproblem. Bold values denote relevant results discussed in the text and Table 5.

| | | Method | SP1 | SP2 | SP3 | SP4 | SP5 | SP6 | SP7 |
|---|---|---|---|---|---|---|---|---|---|
| Objectives | $m$ (g) | | 378 | 378 | 378 | 378 | 378 | 378 | 378 |
| | $\sigma_{xy}$ (MPa) | FE Analysis | **32.84** | 28.79 | **25.43** | 24.85 | 23.90 | 22.08 | 22.49 |
| | | NN System | 33.15 | 29.89 | 26.50 | 24.66 | 24.16 | 21.80 | 22.05 |
| | | Error (%) | 0.9 | 3.1 | 4.2 | 0.7 | 1.1 | 1.2 | 1.9 |
| | $\epsilon_{yy}$ | FE Analysis | **4.76** | 4.46 | **4.24** | 4.23 | 4.22 | 4.22 | 4.21 |
| | | NN System | 4.78 | 4.57 | 4.16 | 4.17 | 4.17 | 4.35 | 4.23 |
| | | Error (%) | 0.4 | 2.5 | 1.9 | 1.4 | 1.2 | 3.0 | 0.5 |
| Constraints | $FI_{TT}$ | FE Analysis | – | – | – | 0.32 | 0.42 | **0.948** | 0.784 |
| | | NN System | – | – | – | 0.31 | 0.45 | 0.93 | 0.81 |
| | | Error (%) | | | | 6 | 7.1 | 1.9 | 3.3 |
| | $FI_{LC}$ | FE Analysis | **0.996** | 0.64 | 0.61 | 0.58 | 0.47 | **0.996** | 0.87 |
| | | NN System | 0.97 | 0.68 | 0.65 | 0.54 | 0.49 | 0.98 | 0.89 |
| | | Error (%) | 2.6 | 6.2 | 6.5 | 6.9 | 4.2 | 1.6 | 2.3 |
| | $FI_{TC}$ | FE Analysis | **0.978** | 0.80 | 0.36 | – | – | – | – |
| | | NN System | 0.98 | 0.82 | 0.38 | – | – | – | – |
| | | Error (%) | 0.2 | 2.5 | 5.6 | | | | |

**Table 5**
Comparison of the reference and optimal panels for the most restrictive subproblems.

| | | Panel | SP1 | SP3 | SP6 |
|---|---|---|---|---|---|
| Objectives | $m$(g) | Reference panel | 379 | 379 | 379 |
| | | Optimum panel | 378 | 378 | 378 |
| | | Reduction (%) | 0.54 | 0.54 | 0.54 |
| | $\sigma_{xy}$ (MPa) | Reference panel | 35.52 | 27.06 | 23.24 |
| | | Optimum panel | 32.84 | 25.43 | 22.08 |
| | | Reduction (%) | 7.55 | 6.02 | 4.99 |
| | $\epsilon_{yy}$ | Reference panel | 5.09 | 4.46 | 4.37 |
| | | Optimum panel | 4.76 | 4.24 | 4.22 |
| | | Reduction (%) | 6.48 | 4.93 | 3.43 |

the response of 120 FE analysis for each sub-problem to achieve a good performance of the system. A data processing MSE of about $10^{-4}$ is obtained.

### 3.2. Genetic algorithm

A variant of the algorithm Non-dominated Sorting Genetic Algorithm II (NSGA-II) [35] is used to solve the formulated problem by the Toolbox for Matlab (Global Optimization). It is one of the results of the evolution of the GA and is based on the application of elitism preserving the use of Pareto front. This elitism is controlled by two options: the *Pareto fraction* and *crowding distance measure* functions. The first, limits the number of individuals on the Pareto front and the distance function helps to maintain diversity on a front by favoring individuals that are relatively far away on the front.

The fitness function, which measures the genetic informations of each individual, is composed of the different objectives and the constraints. A penalty method is used to describe the constraints, reported in Eq. (4). The individuals with better characteristics survive during the evaluation process.

The genetic search is performed with a population size of 75 members, generated randomly, with a 'genotype' function as crowding distance measure and the value of the Pareto fraction is set as 0.5.

## 4. Results and discussion

The GA converged after 33 generations and required 1701 fitness function evaluations. A considerable reduction of the computational cost is achieved with the optimization procedure proposed. In fact, to obtain the optimal configuration, 120 FE analysis for each subproblem were performed in a total computational time of about 35 h. The used computer is a DELL Precision T1500 with an Intel® Core™ i5 CPU with 2.67 GHz, 4 GB of RAM, Windows 7 x64 Edition. The CPU time required by the ANN training process was approximately 25 min, while the computational cost for optimization was about 8 min. However, a direct optimization using GA coupled with FE analysis supposes about 1701 different simulations for each subproblem, which means roughly 500 h of computational time.

The optimal panel has been selected between all those solutions of the Pareto front such as each objective function has the same weight. This panel is characterized by a mass of 378 g and the following dimensions: $x_1$ = 26.397 mm, $x_2$ = 21.404 mm and $x_3$ = 90.23 mm.

The solution obtained using the ANN modeling is compared with the FE modeling for each subproblem as shown in Table 4.

In turn, all the failure indexes of LaRC criterion are verified to be lower than 1. For this parameters, the most restrictive problems have been the SP1 for temperature increase and SP3 and SP6 for temperature decrease. In comparison with the reference panel,

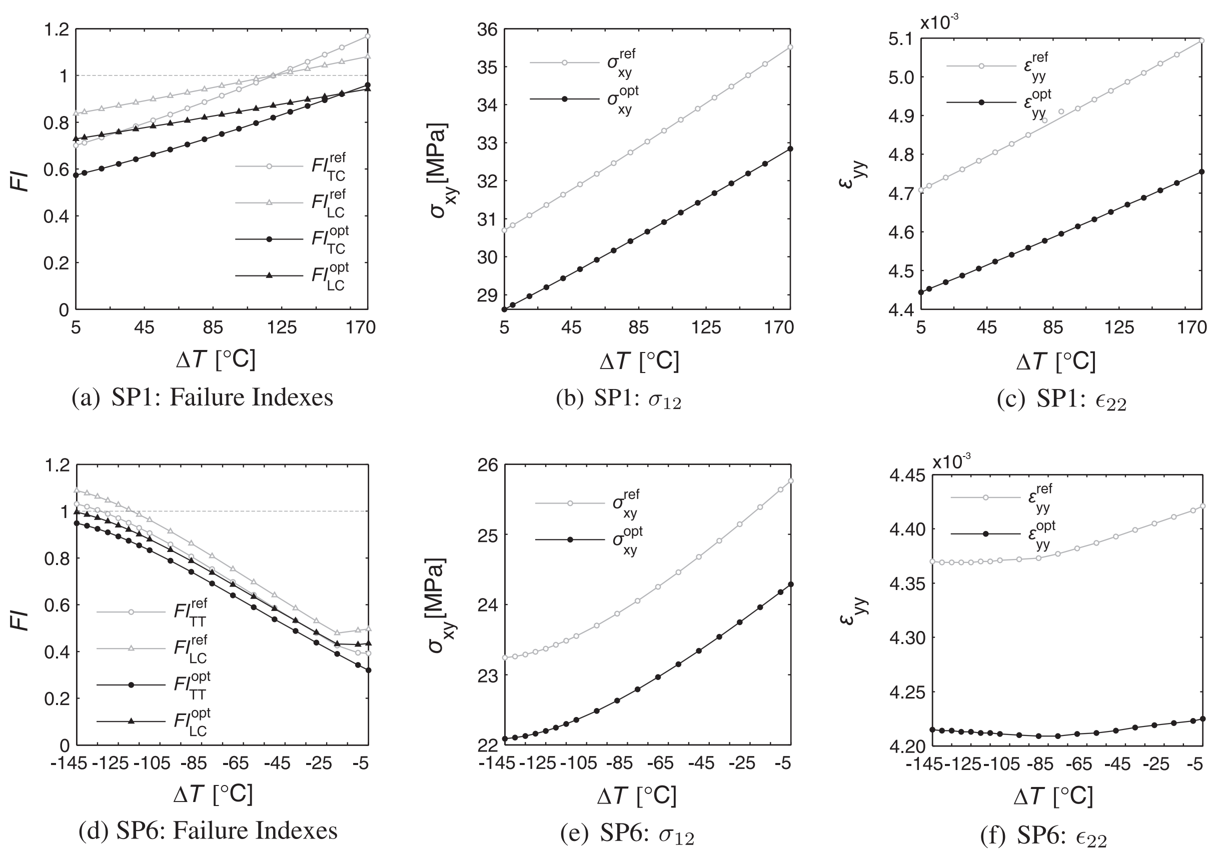

(a) SP1: Failure Indexes (b) SP1: $\sigma_{12}$ (c) SP1: $\epsilon_{22}$

(d) SP6: Failure Indexes (e) SP6: $\sigma_{12}$ (f) SP6: $\epsilon_{22}$

**Fig. 4.** Comparison between reference and optimal panels.

the reduction in mass is 0.54%, and the hygrothermal strain and the tensions between the stiffeners and the skin are reduced about 6.48–3.43% and 7.55–4.99% respectively depending on the subproblem (Table 5).

Positive and negative temperature increments of five degrees are considered for each interval in Fig. 4, where the comparison between these panels is shown for the extreme temperature cases. In both cases, the reference panel breaks as failure indexes values indicate in Fig. 4a and d while the optimal panel shows a good performance and the strain and the tension between the stiffeners and the skin are considerably reduced.

## 5. Conclusions

An optimization procedure for stiffened panels under mechanical and hygrothermal loads has been developed. This procedure consists of the interaction between an ANN system and a GA with the purpose of reducing the computational cost that could reach a direct optimization using FE analysis to obtain the response of the panel. For the correct definition of the optimization problem, the behavior of a reference panel has been analyzed by means of FE with the aim of selecting the most significant objectives and constraints for the possible load states.

A set of seven subproblems characterized by different temperature ranges and moisture presence was considered in the optimization procedure. This decomposition of the initial problem in several subproblems helps to analyze the hygrothermal effects with negative or positive thermal variations and to find the optimal panel for the maximum number of load cases at which these structural elements can be subject. However, the implementation of different subproblems increases the computational cost in the optimization problem.

The use of ANN systems can increase the speed of the optimization processes, reducing the computational cost about 92.8%. The drawback of these tools is the time required to design its architecture to obtain the suitable learning, which can be higher in specific terms and affect the optimization results. However, comparing the optimal panel behavior calculated with FE analysis and ANN system, it can observed that is suitable for all subproblems and is able to reduce the several objectives satisfying the considered constraints. Comparing the optimal and reference panels, the mass is reduced about 0.54% and the hygrothermal strain and tension between stringers and skin are decreased until 6.48% and 7.55% respectively in specific load cases.

In conclusion, ANN and GA reduce the computational cost with suitable accuracy and can help to implement several load states to minimize the global problem. These tools can be used in engineering applications with a unique or various ANN systems. On the other hand, to reduce the time required to train the ANN and replace the problematic trial-and-error approach, a GA system could be used to find the optimal internal architecture.

## Acknowledgments

The authors acknowledge the financial support of the Spanish Government under the Project DPI2009-08048. The first author would like to thank Spanish Government for the FPI pre-doctoral Grant BES-2010-042387.

## References

[1] Kaufmann M, Zenkert D, Mattei C. Cost optimization of composite aircraft structures including variable laminate qualities. Compos Sci Technol 2008;68(13):2748–54.
[2] Rikards R, Abramovich H, Kalnins K, Auzins J. Surrogate modeling in design optimization of stiffened composite shells. Compos Struct 2006;73(2):244–51.
[3] Badran SF, Nassef AO, Metwalli SM. Y-stiffened panel multi-objective optimization using genetic algorithm. Thin Wall Struct 2009;47(11):1331–42.
[4] Irisarri FX, Bassir DH, Carrere N, Maire JF. Multiobjective stacking sequence optimization for laminated composite structures. Compos Sci Technol 2009;69(7-8):983–90.
[5] Irisarri FX, Laurin F, Leroy FH, Maire JF. Computational strategy for multiobjective optimization of composite stiffened panels. Compos Struct 2011;93(3):1158–67.
[6] Todoroki A, Ishikawa T. Design of experiments for stacking sequence optimizations with genetic algorithm using response surface approximation. Compos Struct 2004;64(3-4):349–57.
[7] Todoroki A, Sekishiro M. Stacking sequence optimization to maximize the buckling load of blade-stiffened panels with strength constraints using the iterative fractal branch and bound method. Compos Part B: Eng 2008;39(5):842–50.
[8] Todoroki A, Sekishiro M. New iteration fractal branch and bound method for stacking sequence optimizations of multiple laminates. Compos Struct 2007;81(3):419–26.
[9] Wang W, Guo S, Chang N, Yang W. Optimum buckling design of composite stiffened panels using ant colony algorithm. Compos Struct 2010;92(3):712–9.
[10] Gigliotti M, Riccio A, Iuspa L, Scaramuzzino F, Mormile L. Weight optimisation of damage resistant composite panels with a posteriori cost evaluation. Compos Struct 2009;88(2):312–22.
[11] Nagendra S, Jestin D, Gürdal Z, Haftka RT, Watson LT. Improved genetic algorithm for the design of stiffened composite panels. Comput Struct 1996;58(3):543–55.
[12] de Faria A, de Almeida S. Buckling optimization of plates with variable thickness subjected to nonuniform uncertain loads. Int J Solids Struct 2003;40(15):3955–66.
[13] Topal U, Uzman U. Thermal buckling load optimization of laminated composite plates. Thin Wall Struct 2008;46(6):667–75.
[14] Young-Shin L, Yeol-Wha L, Myung-Seog Y, Bock-Sun P. Optimal design of thick laminated for maximum thermal buckling load. J Therm Stresses 1999;22(3):259–73.
[15] Ijsselmuiden ST, Abdalla M, Gnrdal Z. Thermomechanical design optimization of variable stiffness composite panels for buckling. J Therm Stresses 2010;33(10):977–92.
[16] Cho HK. Optimization of dynamic behaviors of an orthotropic composite shell subjected to hygrothermal environment. Finite Elem Anal Des 2009;45(11):852–60.
[17] Boukhoulda BF, Adda-Bedia E, Madani K. The effect of fiber orientation angle in composite materials on moisture absorption and material degradation after hygrothermal ageing. Compos Struct 2006;74(4):406–18.
[18] He Y. In-situ characterization of moisture absorption–desorption and hygroscopic swelling behavior of an underfill material. In: Electronic components and technology conference; 2011. p. 375–86.
[19] Vaddadi P, Nakamura T, Singh R. Inverse analysis to determine hygrothermal properties in fiber reinforced composites. J Compos Mater 2007;41:309–34.
[20] Chang TW, Tsai CL, Yeih W, Chang JJ. Tracking the moisture expansion of carbon/epoxy composite exposed to varying humidity. J Compos Mater 2008;42(2):431–43.
[21] Orifici AC, Thomson RS, Herszberg I, Weller T, Degenhardt R, Bayandor J. An analysis methodology for failure in postbuckling skin-stiffener interfaces. Compos Struct 2008;86(1-3):186–93.
[22] Orifici AC, Shah SA, Herszberg I, Kotler A, Weller T. Failure analysis in postbuckled composite T-sections. Compos Struct 2008;86(1–3):146–53.
[23] Holland J. Adaptation in natural and artificial systems: an introductory analysis with applications to biology, control, and artificial intelligence. MIT Press; 1975.
[24] Goldberg DE. Genetic algorithms in search, optimization and machine learning. Addison-Wesley Pub. Co.; 1989.
[25] Bisagni C, Lanzi L. Post-buckling optimisation of composite stiffened panels using neural networks. Compos Struct 2002;58(2):237–47.
[26] Lanzi L, Bisagni C, Ricci S. Neural network systems to reproduce crash behavior of structural components. Comput Struct 2004;82(1):93–108.
[27] ABAQUS version 6.9: ABAQUS User's manual. SIMULIA World Headquarters, 166 Valley Street, Providence, RI 02909, USA; 2009.
[28] Barbero EJ. Introduction to composite materials design. 2nd ed. CRC Press. Taylor & Francis Group; 2011.
[29] Mayugo JA. Proyecto: ensayo virtual y supervisión estructural de revestimientos reforzados con larguerillos de fibra de carbono EVISER IT-01, ref: TRA2006-15718-C02-01/TAIR. AMADE. Universitat de Girona; 2006–2009.
[30] Dávila CG, Camanho PP, Rose CA. Failure criteria for FRP laminates. J Compos Mater 2005;39:323–45.
[31] MIL-HDBK-17-3F (Military Handbook). Composite materials handbook: polymer matrix composites materials usage, design, and analysis, vol. 3. Department of Defense of USA; 2002.
[32] Müller B, Reinhardt J. Neural networks. An introduction. Berlin Heidelberg New York: Springer-Verlag; 1995.
[33] MATLAB. Using MATLAB manual. The Math Works Inc. Natick, MA; 1999.
[34] Dennis Jr JE, Schnabel RB. Numerical methods for unconstrained optimization and nonlinear equations. SIAM, Philadelphia; 1983. 1996.
[35] Deb K. Multi-objective optimization using evolutionary algorithms. John Wiley & Sons; 2001.
[36] Valery V Vasiliev, Evgeny V Morozov. Advanced mechanics of composite materials; 2007.